



Intelligent fault monitoring and reliability analysis in safety-critical systems of nuclear power plants using SIAO-CNN-ORNN

Kumar Gaurav¹ · Binod Kumar Singh¹ · Vinay Kumar^{1,2}

Received: 10 May 2023 / Revised: 5 October 2023 / Accepted: 21 November 2023

© The Author(s), under exclusive licence to Springer Science+Business Media, LLC, part of Springer Nature 2024

Abstract

Nuclear power plants' instrumentation and control systems (I&Cs) are essential for guaranteeing secure and dependable operations. If these systems fail, there could be serious accidents, radiation exposure risks, and environmental damage. To avoid catastrophic outcomes, the dependability of I&C systems in NPPs is of the utmost importance. With the help of the suggested methodology, the instrumentation and control system's dependability are examined efficiently. This paper aims to employ deep learning models to analyze the I&C system's reliability. A novel fault monitoring system with reliability analysis of Safety-Critical Systems (SCS) is introduced based on the hybrid deep learning (HDL) Model. The hybrid deep learning model is developed based on a convolutional neural network (CNN) and an optimized Recurrent Neural Network (RNN) (CNN-ORNN). In addition to that, a Weighted Kurtosis and Skewness (WKS)-based Aquila Optimizer Algorithm (AOA) is developed to enhance the feature learning strategy. The automated feature learning is achieved in the HDL, where a new Self-Improved Aquila Optimizer (SIAO) is utilized for an optimized Recurrent Neural Network. SIAO is a conceptual enhancement of the standard Aquila optimizer. To demonstrate the assessment, a nuclear power plant's isolation condenser system is utilized and implemented in Matlab. Moreover, the performance of the proposed model is evaluated based on the performance matrices, i.e., accuracy, specificity, sensitivity, False Positive Rate (FPR), and False Negative Rate (FNR). In addition, reliability is also utilized because it is a major parameter for evaluating the performance of the proposed model for I&C systems in NPPs.

Keywords Safety-critical system · Reliability prediction · CNN · RNN · Aquila Optimizer

✉ Kumar Gaurav
2018rscs013@nitjsr.ac.in

Binod Kumar Singh
bksingh.cse@nitjsr.ac.in

Vinay Kumar
vinay@iiitnr.edu.in

¹ Department of Computer Science and Engineering, National Institute of Technology Jamshedpur, Jamshedpur, Jharkhand, India

² Department of Computer Science and Engineering, Dr. Shyama Prasad Mukherjee International Institute of Information Technology-Naya Raipur, Atal Nagar, Naya Raipur, Chhattisgarh, India

1 Introduction

In the next 50 years, nuclear power plants (NPPs) are likely to play a huge role in electrical energy production, with many being developed internationally, especially in developing nations. Even though new NPP projects are emission-free, increasing plant safety is still their prime priority [1]. Autonomous systems enable the safe functioning of complicated systems that are prone to human mistakes. Guidelines for advanced nuclear power plant designs to utilize these systems are being developed under the guidance of regulatory research. The economical, streamlined boiling water reactor design and tiny modular reactor operation and maintenance performance are examples of current advanced reactor systems that use highly automated intelligent control systems [2]. A key problem is still developing techniques that comply with guidelines for system reliability and stability studies and meet stringent reliability and safety standards. [3]. The digital I&C systems utilized in NPPs have several distinctive characteristics, including fault-tolerant methods like self-diagnosis, which are important for enhancing NPP safety [4]. The approach with the greatest usage is still ANN for creating intelligent fault-detection algorithms in the nuclear energy sector. The convolutional layer's local connections and weight-sharing properties effectively extract spatial properties and edge information from the input matrix [5]. Analyzing the reliability of safety-critical systems is a challenging task due to their low failure rates. Nevertheless, the failure of these systems can result in severe consequences, including environmental harm, economic loss, and human injuries or fatalities. Researchers are continually exploring various modelling techniques, including Software Reliability Growth Models and Reliability Block Diagrams, to address the reliability of SCS and propose effective solutions. [6].

The International Atomic Energy Agency (IAEA) recommends that any NPP I&C simulator should possess the certain desirable characteristics to ensure an accurate progress assessment. However, "fine-tuning" the simulator can be a time-consuming, costly, and technically challenging process, despite modelling predicting that the NPP's performance will be in line with the "as-designed" plant [7]. Additionally, modelling is often regarded as an art rather than a precise science.

Safety is always given top priority in NPPs, regardless of the expense. For the licensing of electronic systems in both current and future NPPs, regulatory bodies are demanding software with almost zero defects. Software that is considered to be safety-critical must have a probability density of less than per demand [8]. The extensive stock of radioactive fission products produced during nuclear fission in NPPs poses a risk to the public, and even after the NPP is shut down, the disintegration of these radioactive elements still produces a large amount of heat [9].

The integration of microcomputer electronic systems into NPP safety I&C systems has led to a significant challenge in incorporating their characteristics into the PRA model of NPPs. The main aim is to assess the reliability of digital systems and understand their potential risk to NPP safety [10]. In the case of an NPP, inspections are crucial procedures that require highly qualified personnel and specialised tools. Two different types of inspections, Pre-Service Inspections and periodic inspections, are typically carried out amid fuel refills [11]. To achieve the high level of reliability required for safety system applications and to avoid the possibility of factors not fulfilling preset safety criteria, advertising practices are now being updated [12].

The LSTM and VAE combo efficiently recognise aberrant circumstances and validate the diagnostic outcomes of the LSTM network. A diagnostic algorithm can be used to locate unknown events, validate diagnostic findings, and make final diagnoses to increase the accuracy of diagnosis [13]. To track the dependability of automatic control systems and components in nuclear power plants, an expansion of the GO-FLOW

technique is used to enhance the GO-FLOW model, and the analysis framework supports modular modelling and improves model readability by employing a hierarchical modelling method [14]. He [15] presents a cost-effective approach for evaluating the SV's dependability using small sample tests and, based on rigorous FMEA analysis, identifies the cartridge and mechanical elements as the main contributors to SV reliability.

According to this study, deep learning models may be used to assess the I&C system's dependability. A novel Hybrid DL Model for SCS Reliability Analysis will be provided in this research study. The suggested model has four main steps: collecting data, cleaning up the acquired data, identifying pertinent characteristics, and estimating the data's trustworthiness.

The manuscript begins with the introduction in Section 1, followed by Section 2, which is the literature survey. This section covers some of the related works reviewed in our article, including the problem statement and comparison table. The proposed approach is presented in Section 3. Section 4 covers the results and discussion, which also includes a comparison of the results to existing data and performance indicators. Section 5 concludes the manuscript by summarising the work in light of the results and suggesting areas for future research.

1.1 The foremost contribution of this work

The foremost contributions of this article are as follows:

- The article recommends using DL models to assess the reliability of the I&C system.
- A novel reliability analysis of SCS will be presented using a hybrid deep learning model.
- The predicted prototype consists of four stages: data acquisition, data pre-processing, feature extraction, fault prediction, and reliability analysis.
- The proposed hybrid model, combining CNN with an optimized RNN, will utilize the Self-Improved Aquila Optimizer. This novel meta-heuristic optimization model aims to modify the weight function of the RNN for improved performance.
- A new algorithm based on SIAO called Weighted Kurtosis and Skewness (WKS) is introduced to improve the feature learning performance.

2 Literature review

This section reviews several studies that deal with SCS reliability analysis using hybrid deep learning methods.

In 2015, Kumar and Singh et al. [16] proposed the Reliability modelling of SCS Communication within an NPP that has been digitised. The purpose of this research was to create quantitative plans for addressing different types of network breakdowns and identify conditions that could pose a risk to communication networks connecting GCs and LCs. The fault-tree model for ESF-CCS signal failure was developed by the researchers to predict the effects of network communication faults in a confined spray actuation signal condition for the case study. After constructing a detailed architecture of ESF-CCS, the fault-tree model could be applied to various ESF signal conditions for network communication between GCs and LCs.

In 2015, Lee and Kim et al. [17] provided a model-based methodology for building and verifying FPGA-based reactor protection systems (RPS). The proposed method consisted of several stages, such as analysing requirements, developing enhanced functional flow block diagram (EFFBD) models, creating finite state machines with data path (FSMD) models, developing HDL code, and verifying layout. The effectiveness of the proposed methods in

improving the design verification processes for safety-critical functions was demonstrated in RPS by applying them to bistable fixed-setpoint trip logic algorithms as a case study. Utilising VHDL, MATLAB/Simulink co-simulation, and FPGA hardware test beds, the design verification stages also included unit tests, module tests, and integration tests. The findings demonstrated that the suggested method might enhance design verification procedures while lessening the demand for demanding V&V activities in FPGA-based safety-critical I&C systems for NPPs. Insights into fault-tree modelling for network failure in digital I&C systems and quantification of the risk effect of network failure in safety-critical information transmission in NPPs are the main goals of the project. After creating a thorough ESF-CCS architecture, subsequent research will expand the created fault-tree model to incorporate network communication between GCs and LCs under various ESF signal situations.

In 2017, Singh and Rajput et al. [18] utilised stochastic modelling to analyse the availability of the NPP's safety-critical and control systems. A novel methodology has been introduced to analyse the availability of an NPP's Digital Feed Water Control System by considering the upkeep and repair of the main steam safety valves. The long-term ageing and dependability of the cables are evaluated using conventional methods, which are expensive and time-consuming accelerated life testing (ALT) procedures. The results showed that ANNs can estimate the dependability of I&C cables properly with the right training techniques and network design without the requirement for significant accelerated life testing. The system was modelled using Stochastic Petri nets to capture all system demands as well as common-cause failures and partial malfunctions of its subsystems. Among 10 sample sizes, the accuracy range of ANN varies as follows: the mean is 146639.7 and the standard deviation is 463689.16.

In 2018, Santosh et al. [19] analysed the effects of component reliability changes in safety-critical systems. The effectiveness and theoretical foundation of the proposed technique were revealed and validated using an actual case study of an NPP system. Nuclear power plants commonly use systems composed of multiple parts that perform different tasks. Therefore, the statistical parameters impacting the analysis of change in component reliability in safety-critical systems are the mean of 15.7 and the Standard deviation of 2.98, respectively.

In 2019, Singh et al. [20] proposed an imperative for nuclear safety software for digital I&C systems: reliability testing. An engineering method for identifying the vulnerability factors that affect the DI&C system software life cycle's dependability was studied. A novel strategy for transforming the CAE method into a Bayesian Brief Network was developed, which involved extracting the most sensitive components of the DI&C system through sensitivity analysis using three different reasoning techniques. Therefore, dynamic reliability analysis with digital I&C systems is 0.99603.

In 2019, Ahmed et al. [21] presented utilizing Petri nets to check NPP safety-critical and control systems. A method was developed to perform a performance evaluation of safety-critical and control systems to aid in risk estimation. Petri nets were extended to estimate performability and guarantee the requirements for system dependability. The method was demonstrated using a case study of an NPP. The accuracy of Energy Complexes consisting of Hydro and Nuclear Power Plants with Low Power Nuclear Reactors is 98.74.

In 2019, Singh and Singh [22]. discussed various varieties of reliability assessments, including fault tree analysis, Markov modelling, and reliability predictions. These investigations, which examine several facets of system dependability, are connected. Values for each board's or module's failure rate serve as the fundamental inputs for computing system reliability and availability. A set of VME bus-based microcomputer boards with a PowerPC processor have been planned and developed by RCnD for future systems of new plants and

significant upgrades of current plants. Hardware, software, and human reliability (O&M activities) make up the three parts of an integrated CBS's overall system dependability.

In 2019, Liu et al. [23] analysed the reliability tool called "Relex Reliability Studio 2008," which was used to estimate the failure rate (FR) for the microcomputer boards. The system is built using the MIL-STD-217 Plus approach. Hardware reliability analysis has reached a point where quantitative estimation is feasible, and analysis tools, including these databases, are also readily accessible in the marketplace.

In 2020, Kumar et al. [24] have proposed an approach for early prediction of software reliability using stochastic modelling for feedwater systems. This approach addresses the unrealistic assumption of transition probabilities in the Markov chain made by earlier researchers. However, this model is based on the observable states of the system, and there is a possibility of missing out on undesirable scenarios that may happen in the future. Hence, devising a model that can embed the development characteristics of the software will give more accurate results.

In 2022, Tripathi et al. [25] discussed how Safety-critical systems (SCSs) of nuclear power plants (NPPs) are being designed and developed to meet high dependability requirements. Fault tree analysis (FTA) is widely used for the risk and reliability analysis of NPPs. However, fault trees (FTs) are static and have only limited capability to represent dynamic systems. FTA is also not capable of modelling non-binary logic or the system's evolution over time. Dynamic reliability methods are being developed to deal with such limitations. Time series Markov chains and dynamic flow graph methodology are the dynamic reliability methods that alternate to traditional FTA and can be used for system performance analysis.

2.1 Problem statement

The following Table 1 highlights some of the limitations existing in the previous works related to reliability.

3 Proposed methodology

The goal of our study is to monitor the fault to enhance the reliability of NPP I&C systems using a quantitative approach.

3.1 Reliability analysis of safety-critical system

Due to the difficulty in predicting the occurrence and timing of failures, failure is one of the aspects of uncertainty in SCS. Fault prediction and reliability analysis can answer the question of whether or not a system will last for a particular amount of time. If a system is functioning properly at zero time, its reliability is the conditional probability that it won't fail in a specified amount of time (the initial time). The safety of the system will be high if the system's reliability is high. Safety and dependability seem to be synonymous; however, safety is primarily concerned with the threat to the environment and human life, whereas reliability focuses on the successful operation of a system for a given amount of time. The following shows the significant steps of the novel fault monitoring and reliability analysis of NPP.

The basic diagram for the proposed method is shown in Fig. 1. It can be described as follows:

Table 1 Problem statement

Author/ year	Methodology	Aim /objective	Disadvantage
Yang Jun, Zou Bowen, yang Ming/2019	Markov/CCMT search engine platform	Modelling and analyzing the reliability of dynamic systems	Due to its enormous computational complexity, the "state-space explosion problem" restricts reliability calculations for safety-critical systems
Jie he, Tangtang bao, Jie Wu, Ge shao, Dongxiao du, Xuhui ie, Qin fang Zhang/2018	Monte Carlo approach	Assessing the SV's reliability	Ignoring completeness and model uncertainty in PRA can underestimate the overall risk assessment
A. Manish Tripathi a, ff. b. Lalit Kumar Singh b, c, Suneet Singh /2019 [9]	Fault tree analysis	Dynamic reliability analysis	Only two failure states are considered
He, J., Bao, T., Wu, J., Shao, G., Du, D., Le, X. and Zhang, Q., 2018 [15]	Bayesian inference, Monte Carlo approach	Reliability assessment	Fault tree analysis assumes unlikely independent failure events

- (a) Data acquisition
- (b) Data pre-processing
- (c) Feature extraction
- (d) Fault Monitoring with reliability prediction

3.2 Data acquisition

The proposed reliability prediction model is implemented using a dataset that is related to the trivial modular reactor IP-200 NPP [5]. Precisely, the dataset collection is achieved with the help of the Relap5 tool [37]. The dataset has been obtained based on conditions such as Steady State, Pressurizer PORV stuck open, Steam Generator tube rupture, Feed-water line break, and RCP Failure, where the tolerance rate of each condition is 100%, 100%, 10%, 50%, and 1 out of 4, respectively.

3.3 Data pre-processing

Pre-processing helps to make the RELAP5 dataset, which may have repeated data, null values, missing values, etc. Therefore, the pre-processing step helps to enhance the data so that it can be well performed with the deep learning model for online fault prediction.

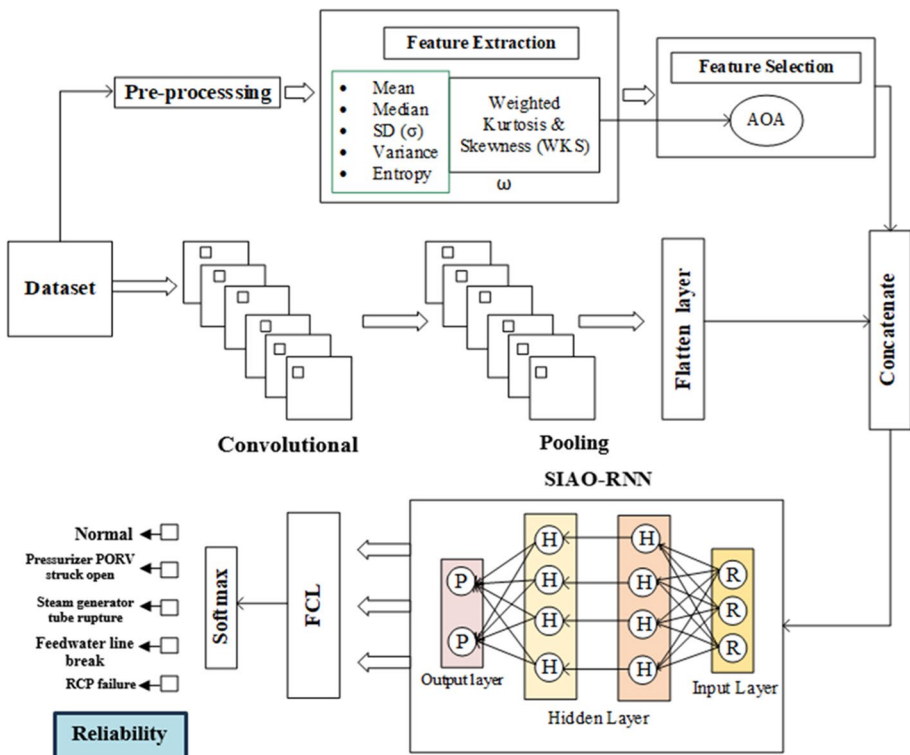


Fig. 1 Overall architecture of the fault prediction framework

During this process, the size of the original RELAP5 dataset will be reduced to a small dataset. Specifically, the dataset related to NPP safety-based RELAP has been contaminated with an abundance of data that may be repeated, irrelevant, or missing. These values are analyzed and properly managed for high-level fault monitoring with the incorporation of a hybrid deep learning approach. Once the pre-processing is done with the RELAP5 dataset, The clearest and most optimal dataset is generated, which can be transferred to the further procedure of feature extraction discussed in the following section.

3.4 Feature extraction

To analyze the I&C system’s reliability in SCS, feature extraction is a real-time technique that transforms the operation data that has already been pre-processed. The dataset is processed with statistical operations for feature extraction in terms of mean, median, SD, variance, and min–max. The Relap5-based IP-200 dataset utilizes higher-order statistical features like skewness, kurtosis, and entropy-based features for high-level feature extraction. Table 2 illustrates the statistical features and the formulas.

Apart from the other features in Table 2, Kurtosis and Skewness are considered the better features. Therefore, the fault and reliability monitoring-based proposed framework introduces improved Kurtosis and Skewness. The improved Kurtosis and improved Skewness are the incorporated weight factors. The optimal weight factors help to enhance the features (Kurtosis (Kt) and Skewness (Sk)), which is to analyze the distribution of data. The mathematical derivation of the weighted kurtosis is shown in Eq. (1).

$$Kt = \frac{\sum_i^N (Y_i - \bar{Y})^4}{(N - 1)\sigma^4} \tag{1}$$

where, Y_i represents the i th distribution’s variable, the mean distribution can be represented as \bar{Y} , N represents the number of variables in the distribution, and σ^2 represents the standard deviation. Similarly, the Skewness is considered a significant feature that can fetch information from the dataset. The mathematical formulation of the Skewness is shown in Eq. (2).

Table 2 Formula for statistical features

Sl. No	Statistical feature	Formula
1	Mean	$\frac{\text{Sum of all values}}{\text{Total number of values}}$
2	Median	$\begin{cases} \frac{l+1}{2}, & \text{for odd} \\ \frac{l}{2}, & \text{for even} \end{cases}$
3	SD (σ)	$\sqrt{\frac{\sum (x_i - \mu)^2}{N}}$
4	Variance	$\frac{\sum (x_i - \mu)^2}{N}$
5	Kurtosis	$Kt = \frac{\sum_i^N (Y_i - \bar{Y})^4}{(N-1)\sigma^4}$
6	Skewness	$Sk = \frac{\sum_i^N (Y_i - \bar{Y})^3}{(N-1)\sigma^3}$
7	Entropy	$\sum_{i=1}^N P_i \log 2 P_i$

$$Sk = \frac{\sum_i^N (Y_i - \bar{Y})^3}{(N-1)\sigma^3} \quad (2)$$

The performance of the “ K_I ” and “ Sk ” is improved by incorporating the weight factor “ ω ” based on the Aquila Optimizer (AO). The proposed Weighted Kurtosis and Skewness (WKS) is shown in Eq. (3) with the “ ω ” factor.

$$WKS = \omega * \frac{\sum_i^N (Y_i - \bar{Y})^4}{(N-1)\sigma^4} + \frac{\sum_i^N (Y_i - \bar{Y})^3}{(N-1)\sigma^3} \quad (3)$$

Moreover, the weight is derived based on a strategy of the Aquila Optimizer Algorithm (AOA). Specifically, the aforementioned equation of the “AO” has been considered for generating the optimal weight. The optimal “ ω ” factor provides a high-level feature that enhances fault prediction through optimal feature learning and prediction. Then the hybrid Deep learning model is incorporated for further processing.

3.5 CNN-ORNN-based fault monitoring

In the hybrid architecture, CNN is the first phase of automated feature learning. CNN provides automated feature learning rather than statistical feature learning. The suggested method, however, offers the benefit of automatic learning with optimized feature learning. The convolution layer in the suggested model incorporates numerous convolution kernels. The role of the convolutional layer is to extract local features from the input data.

The convolutional layer’s function is to extract regional features from the data. Then, $w_{(r,p)}^i$ denotes the weight of i -th convolution kernel at the (r, p) point, and $bias^i$ is the bias of the i -th convolution kernel. Let $a_{r,p,q}$ signify the value of the input matrix at the (p, q) point. Equation (4) can be used to express the value of the i -th node in the output matrix.

$$G(i) = f(\sum_{r=1}^n \sum_{p=1}^n a_{r,p} \times w_{r,p}^i + bias^i) \quad (4)$$

The convolutional layer extracts spatial properties and edge information from the input matrix using its local connections and weight-sharing properties.

3.5.1 Pooling layer

A neural network’s pooling layer uses many pooling core types, including mean pooling and max pooling. In this article, the data is down-sampled only using the max pooling core.

3.5.2 Flatten layer

The data is transferred from the pooling layer to the flattening layer, which transforms the data into one-dimensional data. The output of the convolutional layers is flattened into a 1-dimensional array to get the data ready for the following RNN layer. As a result, a fully connected layer and a lengthy feature vector coupled to the ultimate classification model

are produced. The final layer is linked to the one line that has all of the pixel data. Then the data is transferred into the RNN layer.

3.5.3 RNN layer

The extracted features from the CNN are transferred into RNN layers for dealing with the time series data, especially those related to NPP environmental data. RNN provides higher performance than CNN for dealing with time series data. Figure 2 shows the basic architecture of the RNN model.

A recurrent neural network (RNN) sequentially processes the NPP data to learn. The ability of this sequential process to remember what occurred before the current sequence being processed justifies it. Recurrent means that the output from each time step is used as the input for the subsequent time step. In turn, this enables us to discover long-term dependencies in the training set of data. Layers with memory cells make up an RNN. Due to the advantage of this in RNN, the CNN is incorporated into the RNN for processing time series-based feature vectors. Moreover, the sequential feature vectors of RNN are shared with weights. The weight of the RNN is optimized through a SIAO algorithm. Therefore, optimal weights can be obtained, which enhances prediction performance. Finally, the fully connected layers predict the faults that occur in the NPP environment.

3.5.4 Weighted RNN with SIAO

As discussed, the SIAO algorithm is utilized for optimizing the weight of the RNN, which makes the RNN a better model for fault prediction. This section provides detailed information about the SIAO algorithm for weight optimization of RNN.

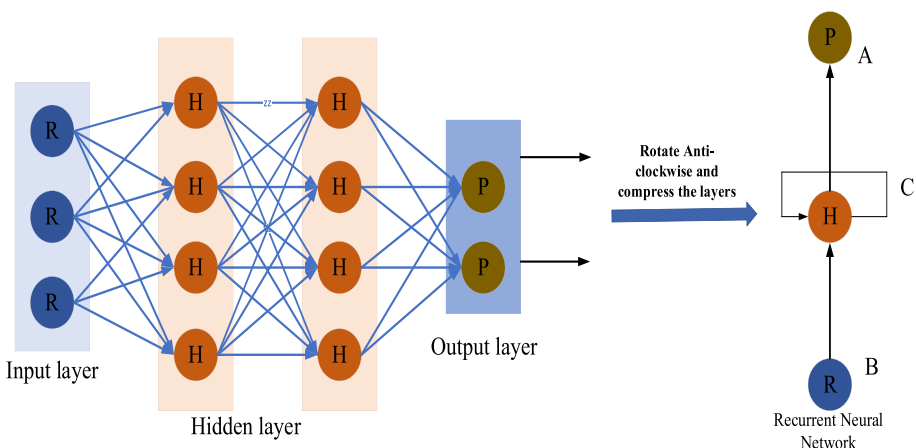


Fig. 2 RNN architecture

3.5.5 Objective function

The SIAO has considered the root mean square error (RMSE) as an objective function of the RNN. The mathematical equation of the RMSE is shown (5)

$$RMSE = \sqrt{\sum_{i=1}^n (y - \bar{y})^2} \quad (5)$$

where y is the actual data, \bar{y} is the predicted data, and n represents the overall data. By minimizing the RMSE, the optimal weights can be identified. Moreover, the proposed SIAO has adopted a chaotic map-based Quality Function (QF) value. The steps of chaotic-based SIAO are discussed in the following section.

3.5.6 Self-improved Aquila Optimization

Step 1: Expanded Exploration X_p In X_p , to locate its prey and pick the best hunting area, the Aquila uses a combination of high soaring and vertical stooping skills. To find the prey during this process, the AO thoroughly searches the search area from a great height.

This behaviour can be expressed mathematically shown in equation (6):

$$X_p(t+1) = X_{best}(t) \times \left(1 - \frac{t}{T_{iter}}\right) + (X_M(t) - X_{best}(t) \times rand) \quad (6)$$

$$X_M(t) = \frac{1}{N_s} \sum_{i=1}^{N_s} X_i(t), \forall i = 1, 2, \dots, D \quad (7)$$

where,

$X_{best}(t)$ best position,

$X_m(t)$ the present iteration's mean position for all Aquilas,

t and T_{iter} the current iteration and the maximum number of iterations,

N_s population size, and.

D dimension size of the problem.

Step 2: Narrowed Exploration X_q The Aquila hunts the majority of the time in narrowed exploration. It descends into the chosen region, flies around the target, and then attacks using short glides. The updated position formula (8) is given below as

$$X_q(t+1) = X_{best}(t) \times Levy_f(D) + X_R(t) + (y - r) \times rand \quad (8)$$

where,

$X_R(t)$ the hawk's random position,

$Levy_f(D)$ the Levy flight function.

The Levy flight function can be expressed as

$$Levy_f(D) = k \times \frac{\mu \times \sigma}{|u|^{\frac{1}{\beta}}} \quad (9)$$

$$\sigma = \left[\frac{s(1 + \beta) \times \sin(\frac{\pi P}{2})}{s(\frac{1+\beta}{2}) \times \beta \times 2^{\frac{\beta-1}{2}}} \right] \quad (10)$$

where, s and β are constants with values of 0.01 and 1.5, respectively, and u and v are random numbers between 0 and 1. The x and y values are used to depict the spiral shape in the search and are derived as shown in Eq. (11):

$$\begin{cases} x = r \times \sin \theta \\ y = r \times \cos \theta \\ r = r_1 + 0.00565 \times D_1 \\ \theta = -\omega \times D_1 + \frac{3 \times \pi}{2} \end{cases} \quad (11)$$

where,

r_1 the search cycles between 1 and 20,

D_1 comprised of integers from 1 to the size D ,

ω 0.005.

Step 3: Expanded exploitation X_r In the third technique, with a vertical descent, the Aquila launches a sneak attack after roughly determining the location of the target. AO makes use of the chosen location to approach and attack the target.

$$X_r(t+1) = (X_{best}(t) - X_M(t)) \times \alpha - rand + ((U_b - L_b) \times RAND + L_b) \times \delta \quad (12)$$

where,

α and δ parameters for exploitation modification set to 0.1, and.

U_b and L_b the upper and lower bounds of the function.

Step 4: Narrowed exploitation X_s The Aquila chases its victim and carefully examines any possible escape routes before finally tackling it on the ground. This is how the Aquila hunts. This hunting behaviour can be mathematically represented as

$$X_s(t+1) = QF \times X_{best}(t) - (H \times XP(t) \times rand) - H_2 \times Levy_f(D) + rand \times H_1 \quad (13)$$

$$QF(t) = t^{2 \times rand - 1 / (1 - T_{iter})^2} \quad (14)$$

$$H_1 = 2 \times rand - 1 \quad (15)$$

$$H_2 = 2 \times (1 - \frac{t}{T_{iter}}) \quad (16)$$

where,

$XP(t)$ current position,

$QF(t)$ quality function value to balance the search strategy.

H_1 Aquila's tracking prey movement parameter is a random number between $[-1, 1]$.

H_2 the flying slope, linearly declines from 2 to 0.

Step 5: Chaotic-based QF The three chaotic-based mathematical formulas have been adopted in the exploitation stage (step 4) instead of the traditional QF function. The chaotic formulas are as follows:

$$1.95 - 2t^{1/4} / T^{1/3} \quad (17)$$

$$1.95 - 2t^{1/3} / T^{1/4} \quad (18)$$

$$0.5 + 2\exp[-(4t/T)^2]. \quad (19)$$

The aforementioned Chaotic QF has been adopted in SIAO; therefore, the performance of SIAO shows better improvement by preventing local optima. At last, the optimized weight concerning minimal RMSE can enhance the RNN and its outcome is transferred into the fully connected layer.

3.5.7 Fully connected layer

For classification purposes, the Softmax activation function is applied to the output of the previous layer, represented by a^{L-1} , along with the weight w^L and bias $bias^L$. As each neuron in the fully connected layer is connected to every neuron in the preceding layer, this approach can be useful for classification.

$$a^L = f(w^L a^{L-1} + bias^L)$$

Finally, the faults of the NPP-based IP-200 are successfully monitored which prevents the NPP environment from severe damage. Figure 3 depicts the hybrid model's architectural framework.

3.6 Maintenance planning

Besides fault monitoring, the proposed model also focuses on reliability analysis. Therefore, the proposed model has analyzed the data in terms of failure occurrence and Mean Time to Failure. The reliability analysis is a significant process to ensure the safety of the NPP environment. The proposed model relies on the IP-200 dataset that was generated using Relap5. In addition to that, the dataset is modified to make it suitable for dynamic reliability analyses. Moreover, the proposed model focuses mainly on analyzing the reliability of the reactor coolant pump (RCP) Failure, steam generator tube rupture, pressurizer PORV stuck open, and normal (steady state). Therefore, the failure rate is determined based on the mathematical calculations shown in (20):

$$\text{Failure Rate } (\lambda) = \frac{\text{Number of Failures}}{\text{Operating Time or Cycles}}. \quad (20)$$

If the system faces any failure after 10 s, the failure rate is estimated as $\frac{1}{10}$, i.e. 0.1. Based on this calculation, reliability can be measured by the following calculation.

$$\text{Reliability} = 1 - \lambda. \quad (21)$$

For instance, if the failure rate is identified as 0.1, it can be subtracted from 1, i.e., $1 - 0.1$. So, the result will be 0.9 at that instant of fault or failure detection. In this proposed work, the failure rate per hour is estimated to determine the possibility of failure in different periods. Therefore, the total number of failures is divided by the overall operating time to determine the failure rate shown in (22),

$$\text{Failure Rate hour } (\lambda) = \frac{\text{Number of Failures per hour}}{\text{overall Operating Time}}. \quad (22)$$

Since the computation of reliability is in the dynamic environment (NPP), the mathematical formulation of the failure rate is derived as follows:

$$\lambda = n / [d * (T) + \sum_{i=1}^n x_i] \quad (23)$$

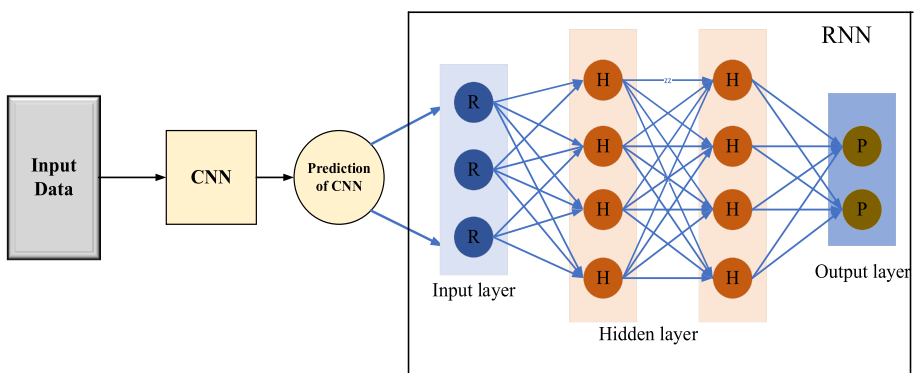


Fig. 3 CNN-RNN architecture

where,

x_i represents the number of failures,
 n is the total failures,
 m represents the total units or machines,
 T is the total operating hours.

Once the failure rate is identified, reliability can be measured based on estimating the Mean Time to Failure (MTTF). The MTTF estimates by taking the inverse of “ λ ” that helps to achieve an average length of an hour before failure. The MTTF can be estimated as follows:

$$MTTF = \frac{1}{\lambda}. \quad (24)$$

From the MTTF, the reliability of the system can be identified based on the equation as follows:

$$Reliability = e^{-T/MTTF} \quad (25)$$

where $e=0.7183$, and T is Total Operating Hours. The $e^{-T/MTTF}$ helps to fetch the reliability of the system. Eventually, the proposed model in NPP can predict the fault as well as ensure reliability.

3.6.1 Safety monitoring

The model provides fault classification and reliability analysis, enabling us to plan maintenance and prevent equipment failures and downtime.

Overall, a deep learning-based fault monitoring system can help improve the reliability and efficiency of equipment such as IP200 by detecting faults early and enabling proactive maintenance [35].

4 Results and discussion

The proposed model is implemented using Matlab 2022b and the Relap5 tool for data collection, and the configuration of the system on which it was implemented is an Intel(R) Core (TM) i3-9100F CPU @ 3.60 GHz and 12 GB of RAM. Finally, the implemented results are evaluated by certain metrics. When compared to earlier methods, the proposed model was quite accurate. Tabulated comparison analysis of the proposed technique with existing literature are presented in Table 7 in the appendix section. Graphs were used to show the performance difference. In Fig. 4, a graph was used to contrast the proposed and existing models' performance on parameters like sensitivity and specificity.

The proposed method was compared with existing techniques, including ORNN, RNN, CNN, Bi-LSTM, and LSTM. It was found to outperform these techniques in terms of sensitivity, specificity, and accuracy. Specifically, the sensitivity value of the proposed method begins at 0.95%, while the values for ORNN, RNN, CNN, Bi-LSTM, and LSTM are 0.93%, 0.89%, 0.87%, 0.85%, and 0.78%, respectively.

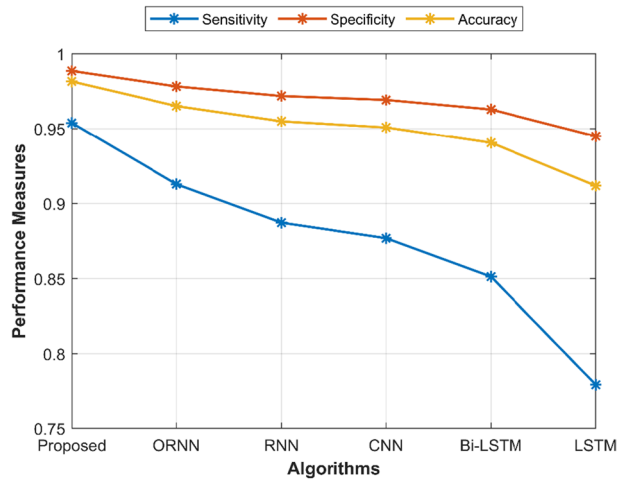
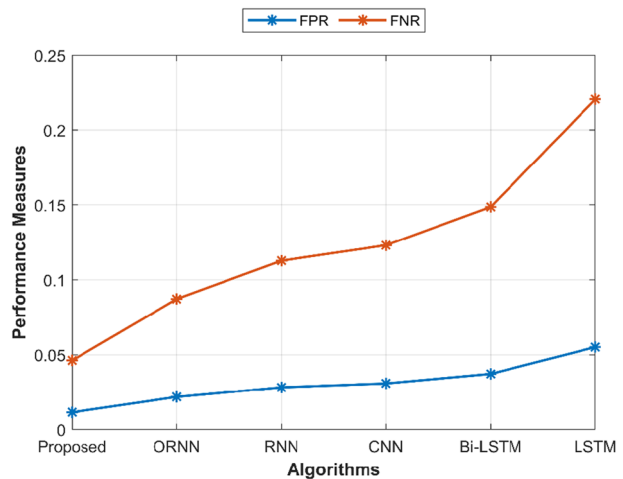
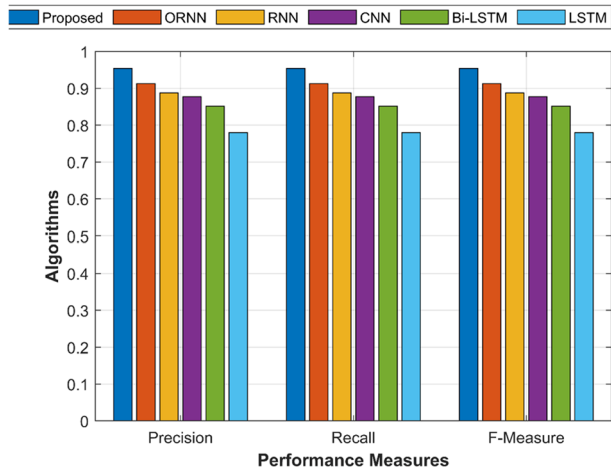
Fig. 4 Comparison of sensitivity, specificity and accuracy**Fig. 5** Comparison of FPR and FNR

Figure 5 shows a graphic representation of the FPR and FNR performance metrics for both the proposed and current methodologies. The proposed model has a lower FPR and FNR when compared to the approaches that are currently in use.

The performance measures, such as recall and F-Measure, for the suggested and current approaches are shown in Fig. 6. For the proposed ORNN, RNN, CNN, LSTM, and Bi-LSTM, respectively, the recall values are 0.953846, 0.912821, 0.887179, 0.876923, 0.851282, and 0.779487; 0.953846, 0.912821, 0.887179, 0.876923, 0.851282, and 0.779487 are F-Measure values. When compared to currently used techniques, the proposed model displays improved recall in Fig. 7.

The performance measures, such as NPV and MCC, for the suggested and current approaches are shown in Fig. 7. For the proposed ORNN, RNN, CNN, Bi-LSTM, and LSTM, respectively, the NPV values are 0.988462, 0.978205, 0.971795, 0.969231, and 0.962821, and the MCC values are 0.942308, 0.891026, 0.858974, 0.846154, 0.814103,

Fig. 6 Comparison of precision, recall and F- Measure

and 0.724359. When compared to currently used techniques, the suggested model displays improved NPV and MCC.

As the expanded dataset is divided into five equal folds, we obtain five scattering plots. The training pictures and testing images are different in each fold. We therefore receive five sets of training and testing characteristics as a result of various training and testing samples. The link between the training and testing characteristics is depicted using a scatter plot.

The CNN model's training epoch is set to 10, as the error rate remained constant after that many epochs and the training graph had reached saturation. The CNN model has the maximum accuracy for five folds after 10 epochs, with validation accuracy obtained from each fivefold cross-validation being 92.2%, 95.2%, 95.3%, 90.7%, and 92.2%. Table 3 displays the average validation accuracy, which is 93.12%.

A batch size of 163 is used to fit the training pictures (data) using the CNN model. The CNN model's validation frequency during training is 10.

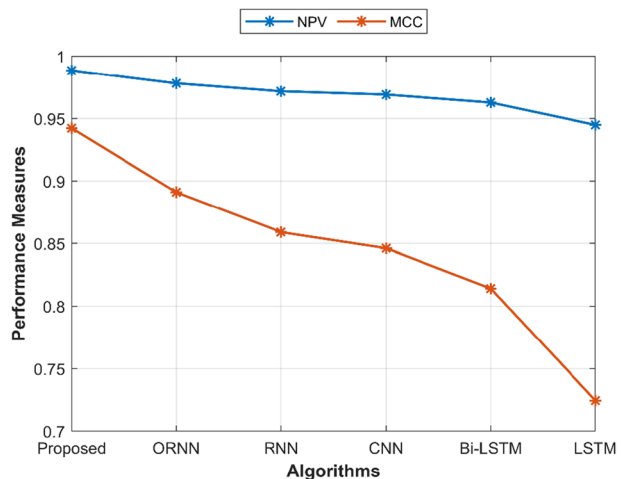
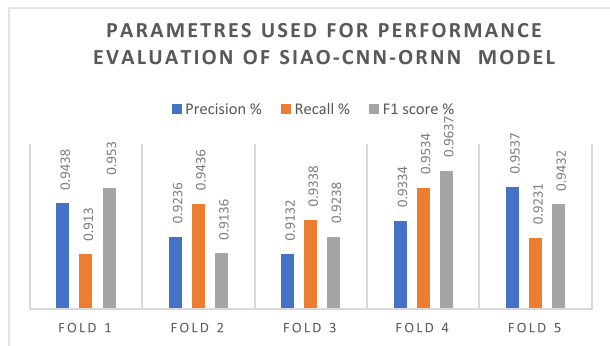
Fig. 7 Comparison of NPV and MCC

Table 3 Accuracy for both CNN, CNN-RNN and SIAO-CNN-ORNN

Fold Number	CNN (%)	CNN-RNN (%)	SIAO-CNN-ORNN (%)
Fold—1	91.1	95.2	98.8
Fold – 2	92.1	93.5	97.4
Fold – 3	95.4	95.8	99.4
Fold – 4	94.7	96.1	99.3
Fold – 5	92.4	94.3	96.8
Average	93.12	96.23	98.74

Fig. 8 Parameters used for performance evaluation of SIAO-CNN-ORNN model

The suggested model runs over 10 epochs, with 25 iterations in each epoch. A learning rate drop factor of 0.2 is used to reduce the learning rate after every 5 epochs. Figure 10 displays the fivefold cross-validation training process. The CNN model's training epoch is set to 10, as the error rate remained constant after that many epochs and the training graph had reached saturation.

The CNN model has the maximum accuracy for five folds after 10 epochs, with validation accuracy obtained from each fivefold cross-validation being 91.1, 92.1, 95.4, 94.7, and 92.4. Table 3 displays the average validation accuracy, which is 93.12%.

The proposed model conducts its operation over a span of ten epochs, with each epoch consisting of 25 iterations. To curtail the learning rate after every five epochs, a drop factor of 0.2 is employed. Figures 8 and 9 showcases the fivefold cross-validation training process. The training epoch of the CNN-RNN model is restricted to ten, as the error rate remained stable beyond that point and the training graph had attained saturation. The CNN-RNN model yields the optimal precision for five folds following ten epochs, with the validation accuracy secured from each fivefold cross-validation attaining 95.2, 93.5, 95.8, 96.1, and 94.3. The fourth table displays the mean validation accuracy, which is determined to be 96.23%.

The SIAO-CNN-ORNN model was trained for 10 epochs, as the error rate did not decrease further beyond that point and the training graph had reached a state of saturation. Upon completion of 10 epochs, the SIAO-CNN-ORNN model demonstrated the highest level of accuracy across five folds, with validation accuracy values of 95.8, 97.4, 99.4, 99.3, and 96.8 obtained from each fivefold cross-validation. The typical attestation correctness, which is revealed in Table 3, was 98.74% (Fig. 10).

Reliability is another crucial parameter for evaluating the performance analysis in safety-critical systems of I&C systems in nuclear power plants [38, 39].

Fig. 9 Parameters used for performance evaluation of CNN-RNN model

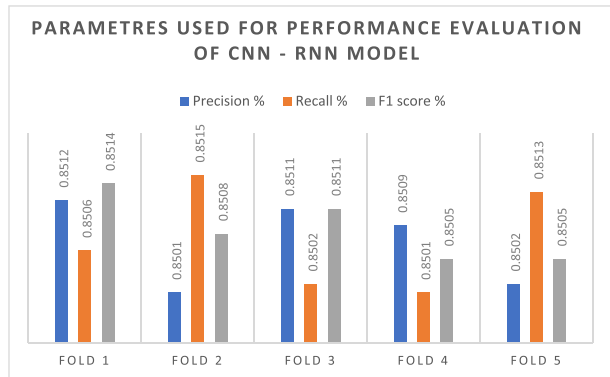


Fig. 10 Parameters used for performance evaluation of the CNN model

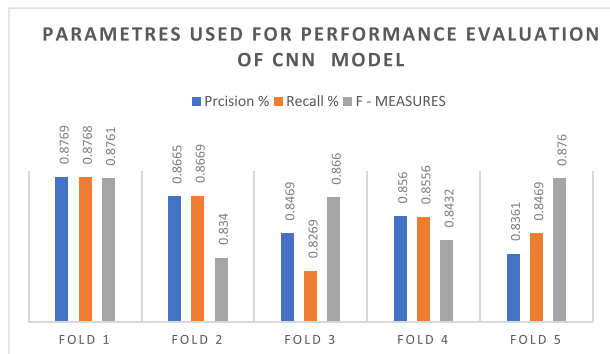


Figure 11 depicts the graphical outcome of the suggested model for reliability calculation in Error Metrics-based analysis in relation to Total Operating Hour. Failure rate per hour decreases abruptly from 5.25 and gradually reduced after 40 h of operation, however the MTTF rate goes from 200 after 20 h and has a linear increase in value, reaching the 1900 range after 200 h of operation. When the operation duration approaches 40, the TMTTP rate drops from 0.105 to 0.085 and then rises exponentially to remain between 0.11 and 0.1. The suggested model's reliability peaked at 0.9175 during the first 40 h of total operation time, then dropped at the same time while the reliability remained between 0.905 to 0.898.

With the consideration of many dependable characteristics, the suggested deep learning approach achieves higher reliability. The analysis of reliability outcomes provided based on different time periods is also shown in Table 6. in the appendix section.

4.1 Comparison with existing techniques

The utilization of SIAO-CNN-ORNN in concurrence with CNN and CNN-RNN models mitigates bias by regularizing the CNN and CNN-RNN outcomes using extracted features. The soft-max activation function is employed for classification by both CNN and CNN-RNN models, but it exclusively operates on training data. Thus, in

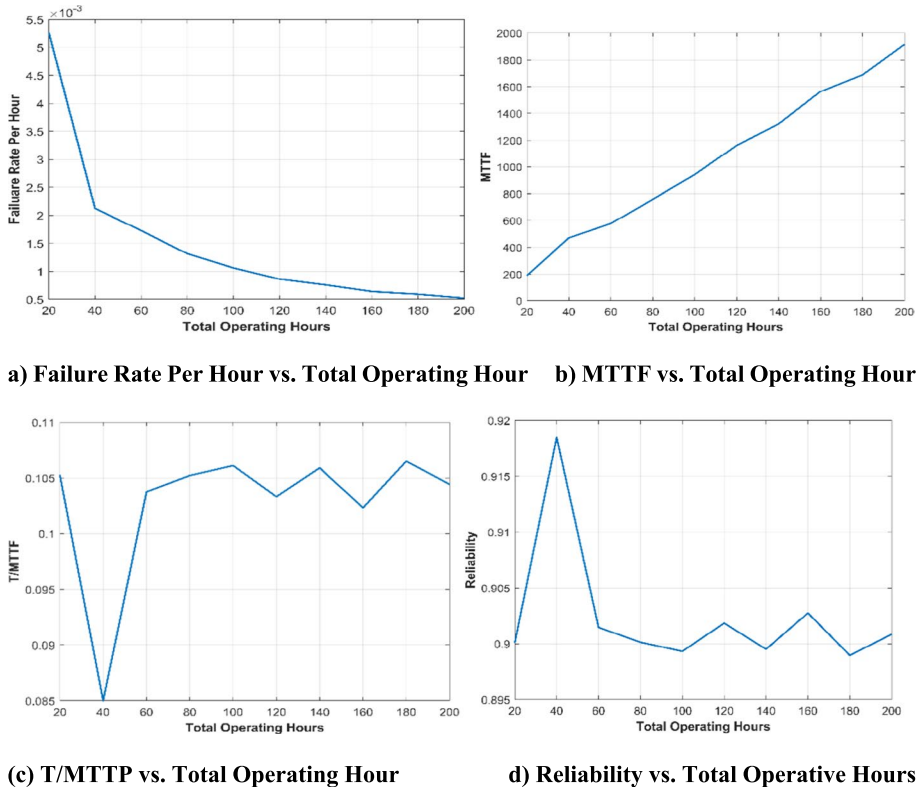


Fig. 11 Comparative graph for reliability calculation

comparison, the proposed SIAO-CNN-ORNN achieves better results than the other existing techniques.

Table 4 shows the comparative analysis in terms of the accuracy of different techniques by considering different literature. Thus, the proposed model is proven to be a better model than the other existing models.

The proposed SIAO-CNN-ORNN method for reliability evaluation in NPP is compared with the existing methods such as Improved TCN, Linear Regression, REPTree, LSTM, ASHRAE, and Pahlev Reliability Index. With error metrics such as Root Mean Squared Error (RMSE), Mean Absolute Error (MAE), Explained Variance Score (EVS), and reliability, Table 5 shows the comparison of the error metrics between the proposed SIAO-CNN-ORNN and the various existing methods.

Table 5 uses multiple evaluation measures to compare how well different strategies perform on the reliability measure. The proposed SIAO-CNN-ORNN method has the lowest root mean square error (RMSE), which is 0.00891, while the Linear Regression and REPTree methods have the greatest R2 Score, which is 0.925. The EVS for the Improved TCN technique is 0.0957, whereas the MAE for the LSTM technique is 0.000966.

The RMSE and MAE values for the ASHRAE and Pahlev Reliability Index methodologies are comparatively high. The RMSE and MAE values for the Pahlev Reliability Index method are comparatively high. The MAE for the CSLSTM method is minimal. The

Table 4 Literature-based accuracy evaluation

References	Technique	Accuracy%
[31]	Petri nets	87
[32]	LSTM	90
[33]	LSTM	94
[34]	SSA-CNN-LSTM	98
[36]	SVM-IPSO	94
Proposed	SIAO-CNN-ORNN	98.74

Table 5 Comparison with existing techniques based on error metrics

Technique	RMSE	MAE	EVS	R ² Score
SIAO-CNN-ORNN	0.00891	0.0312	0.0120	0.0014
Pahlev Reliability Index [26]	0.92	0.85	–	–
CS_LSTM [27]	0.01195	0.000966	–	–
Linear Regression, REPTree [28]	0.009	0.0034	0.0016	0.925
Improved TCN [29]	0.0847	0.0207	0.0957	0.957
ASHRAE [30]	0.75	0.47	0.0025	–

RMSE and MAE values for the Linear Regression and REPTree approaches are relatively low, and they have a good R2 Score but a low EVS. High EVS and R2 scores, high RMSE but low MAE, and an improved TCN method. The ASHRAE approach also has very low EVS and somewhat high RMSE and MAE values.

5 Conclusions

The proposed SIAO-CNN-ORNN framework for fault monitoring and reliability prediction, which utilizes a hybrid deep learning approach, was successfully implemented in MATLAB. This architecture combines a CNN with an optimized RNN, and the novel SIAO algorithm further improves the RNN's performance. In addition to using CNN for automated feature learning, this model employs a novel approach to statistical operations. This includes the application of weighted kurtosis and skewness using the Aquila Optimizer (AO), with weight considerations taken into account. This innovative integration offers significant enhancements in fault prediction and reliability analysis.

Comparing the proposed method to existing models shows that it is better at predicting different kinds of failure, such as the failure of the reactor coolant pump (RCP), the rupture of a steam generator tube, the opening of the pressurizer PORV, and steady (normal) conditions. The results demonstrate the model's effectiveness not only in fault monitoring but also in determining system reliability through mathematical operations.

Lastly, the proposed hybrid model of deep learning and mathematical strategy is effective at detecting faults and enhancing the reliability of safety-critical systems. It is a valuable tool for enhancing the reliability of safety-critical systems owing to its innovative methods and superior performance.

Appendix

The comparison of Performance metrics of different techniques with other literature is tabulated in Table 6. Reliability analysis based on different time periods values are tabulated in Table 7

Table 6 Comparison of performance measures between the proposed approach and existing techniques

Techniques	Sensitivity	specificity	Accuracy	precision	Recall	F-Measures	NPV	FPR	FR	MCC
Proposed CNN-ORNN	0.953846	0.988462	0.981538	0.953846	0.953846	0.953846	0.988462	0.011538	0.046154	0.942308
ORNN	0.912821	0.978205	0.965128	0.912821	0.912821	0.912821	0.978205	0.021795	0.087179	0.891026
RNN	0.887179	0.971795	0.954872	0.887179	0.887179	0.887179	0.971795	0.028205	0.112821	0.858974
CNN	0.876923	0.969231	0.950769	0.876923	0.876923	0.876923	0.969231	0.030769	0.123077	0.846154
Bi-LSTM	0.851282	0.962821	0.940513	0.851282	0.851282	0.851282	0.962821	0.037179	0.148718	0.814103
LSTM	0.779487	0.944872	0.911795	0.779487	0.779487	0.779487	0.944872	0.055128	0.220513	0.724359

Table 7 Reliability analysis based on different time durations

S.No	Time (hours)	Failure Rate per hour	MTTF	T/MTTF	Reliability
1	20	0.005263	190	0.105263	0.900087
1	40	0.002125	470.5	0.085016	0.918497
2	60	0.001729	578.4	0.103734	0.901464
3	80	0.001315	760.4	0.105208	0.900137
4	100	0.001061	942.4	0.106112	0.899323

Abbreviations *I & C*'s: Instrumentation and control systems; *SCS*: Safety-critical systems; *HDL*: Hybrid deep learning; *CNN*: Convolutional neural network; *RNN*: Recurrent Neural Network; *WKS*: Weighted Kurtosis and Skewness; *Kr*: Kurtosis; *Sk*: Skewness; *AOA*: Aquila Optimizer Algorithm; *SIAO*: Self-Improved Aquila Optimizer; *FPR*: False Positive Rate; *FNR*: False Negative Rate; *NPP*: Nuclear Power Plants; *IAEA*: International Atomic Energy Agency; *RPS*: Reactor protection systems; *FSMD*: Finite state machines with data path; *EFFBD*: Enhanced functional flow block diagram; *ANN*: Artificial neural networks; *AO*: Aquila Optimizer; *RMSE*: Root mean square error; *RCP*: Reactor coolant pump; *MAE*: Mean Absolute Error; *EVS*: Explained Variance Score; *RCP*: Reactor coolant pump

Data availability Not Applicable.

Declarations

Conflict of interest The authors declare that we have no conflict of interest.

References

- da Costa RG, de Abreu Mol AC, de Carvalho PVR, Lapa CMF (2011) An efficient Neuro-Fuzzy approach to nuclear power plant transient identification. *Ann Nucl Energy* 38(6):1418–1426
- Lee J, Lin L, Athe P, Dinh N (2021) Development of the machine learning-based safety significant factor inference model for diagnosis in an autonomous control system. *Ann Nucl Energy* 162:108443
- Singh P, Singh LK (2021) Reliability and safety engineering for safety critical systems: an interview study with industry practitioners. *IEEE Trans Reliab* 70(2):643–653
- Lee SJ, Jung W, Yang JE (2016) PSA model with consideration of the effect of fault-tolerant techniques in digital I&C systems. *Ann Nucl Energy* 87:375–384
- Saeed HA, Wang H, Peng M, Hussain A, Nawaz A (2020) Online fault monitoring based on deep neural network & sliding window technique. *Prog Nucl Energy* 121:103236
- Kumar P, Singh LK, Kumar C (2019) An optimized technique for reliability analysis of safety-critical systems: a case study of the nuclear power plant. *Qual Reliab Eng Int* 35(1):461–469
- Kumar P, Singh LK, Kumar C (2020) Performance evaluation of safety-critical systems of nuclear power plant systems. *Nucl Eng Technol* 52(3):560–567
- Cho J, Shin SM, Lee SJ, Jung W (2019) Exhaustive test cases for the software reliability of safety-critical digital systems in nuclear power plants. *Nucl Eng Des* 352:110151
- Tripathi AM, Singh BLK, Singh CS (2020) Dynamic reliability analysis framework for passive safety systems of Nuclear Power Plant. *Ann Nucl Energy* 140:107139
- Lee SH, Lee SJ, Park J, Lee EC, Kang HG (2018) Development of simulation-based testing environment for safety-critical software. *Nucl Eng Technol* 50(4):570–581
- Díaz M, Soler E, Llopis L, Trillo J (2020) Integrating blockchain in safety-critical systems: an application to the nuclear industry. *IEEE Access* 8:190605–190619

12. Lee SH, Son KS, Jung W, Kang HG (2017) Risk assessment of safety data link and network communication in digital safety feature control system of the nuclear power plant. *Ann Nucl Energy* 108:394–405
13. Kim H, Arigi AM, Kim J (2021) Development of a diagnostic algorithm for abnormal situations using long short-term memory and variational autoencoder. *Ann Nucl Energy* 153:108077
14. Lu H, Yang M, Dai X, Li W, Yang J (2019) Reliability modelling by extended GO-FLOW methodology for automatic control components and system at NPP. *Nucl Eng Des* 342:264–275
15. He J, Bao T, Wu J, Shao G, Du D, Le X, Zhang Q (2018) Reliability assessment and data processing techniques of the squib valve in pressurized water NPPs. *Nucl Eng Des* 332:59–69
16. Kumar P, Singh LK, Chaudhari N, Kumar C (2020) Availability analysis of safety-critical and control systems of NPP using stochastic modelling. *Ann Nucl Energy* 147:107657
17. Lee SH, Kim HE, Son KS, Shin SM, Lee SJ, Kang HG (2015) Reliability modelling of safety-critical network communication in a digitalized nuclear power plant. *Reliab Eng Syst Saf* 144:285–295
18. Santhosh TV, Gopika V, Ghosh AK, Fernandes BG (2018) An approach for reliability prediction of instrumentation & control cables by artificial neural networks and Weibull theory for probabilistic safety assessment of NPPs. *Reliab Eng Syst Saf* 170:31–44
19. Singh P, Singh L (2019) Impact analysis of change in component reliabilities in safety-critical systems. *Qual Reliab Eng Int* 35(6):2051–2065
20. Singh LK, Rajput H (2017) Dependability analysis of safety-critical real-time systems by using Petri nets. *IEEE Trans Control Syst Technol* 26(2):415–426
21. Zhukov VV, Pugachev RV, Nyaware BO (2018) Energy complexes consisting of hydro and nuclear power plants with low power nuclear reactors. 2018 International Ural Conference on Green Energy (UralCon), pp 161–166
22. Singh P, Singh L (2019) Verification of safety-critical and control systems of nuclear power plants using Petri nets. *Ann Nucl Energy* 132:584–592
23. Fu Liu, Peizhi Liu (2019) Reliability prediction of an unmanned ground vehicular computer based parts count method. 2019 IEEE International Conference on Unmanned Systems (ICUS), pp 536–541
24. Kumar P, Singh LK, Kumar C (2020) Software reliability analysis for safety-critical and control systems. *Qual Reliab Eng Int* 36(1):340–353
25. Tripathi M, Singh LK, Singh S, Singh P (2022) A comparative study on reliability analysis methods for safety-critical systems using petri-nets and dynamic flowgraph methodology: a case study of nuclear power plant. *IEEE Trans Reliab* 71(2):564–578. <https://doi.org/10.1109/TR.2021.3109059>
26. Norouzi N (2021) The Pahlev Reliability Index: a measurement for the resilience of power generation technologies versus climate change. *Nucl Eng Technol* 53(5):1658–1663
27. Zhang J, Wang X, Zhao C, Bai W, Shen J, Li Y, Pan Z, Duan Y (2020) Application of cost-sensitive LSTM in water level prediction for nuclear reactor pressurizer. *Nucl Eng Technol* 52(7):1429–1435
28. Foshch T, Portela F, Machado J, Maksimov M (2016) Regression models of the nuclear power unit VVER-1000 using data mining techniques. *Procedia Computer Science* 100:253–262
29. Wang H, Peng M, Xu R, Ayodeji A, Xia H (2020) Remaining useful life prediction based on the improved temporal convolutional network for nuclear power plant valves. *Front Energy Res* 8:584463
30. Han O, Li A, Dong X, Li J (2021) Determination of HVAC meteorological parameters for floating nuclear power stations (FNPPs) in the area of the China Sea and its vicinity. *Energy* 233:121084
31. Ahn J, Lee SJ (2020) Deep learning-based procedure compliance check system for nuclear power plant emergency operation. *Nucl Eng Des* 370:110868
32. Lee JH, Yilmaz A, Denning R, Aldemir T (2020) An online operator support tool for severe accident management in nuclear power plants using dynamic event trees and deep learning. *Ann Nucl Energy* 146:107626
33. Yang J, Lee D, Kim J (2019) Accident diagnosis and autonomous control of safety functions during the startup operation of nuclear power plants using LSTM. In *Advances in Artificial Intelligence, Software and Systems Engineering: Joint Proceedings of the AHFE 2018 International Conference on Human Factors in Artificial Intelligence and Social Computing, Software and Systems Engineering, The Human Side of Service Engineering and Human Factors in Energy*, July 21–25, 2018, Loews Sapphire Falls Resort at Universal Studios, Orlando, Florida, USA 9 (pp. 488–499). Springer International Publishing
34. Zhang C, Chen P, Jiang F, Xie J, Yu T (2023) Fault diagnosis of nuclear power plant based on sparrow search algorithm optimized CNN-LSTM neural network. *Energies* 16(6):2934
35. Saeed HA, Peng MJ, Wang H, Zhang BW (2020) Novel fault diagnosis scheme utilizing deep learning networks. *Prog Nucl Energy* 118:103066

36. Wang H, Peng MJ, Hines JW, Zheng GY, Liu YK, Upadhyaya BR (2019) A hybrid fault diagnosis methodology with support vector machine and improved particle swarm optimization for nuclear power plants. *ISA Trans* 95:358–371
37. U.S. Nuclear Regulatory Commission Website [AVAILABLE ONLINE] <https://www.nrc.gov/docs/ML0103/ML010310283.pdf>
38. Mamdikar MR, Kumar V, Bharti S, Singh P (2023) Reliability analysis of safety-critical systems using optimized petri nets. *Prog Nucl Energy* 164:104841.i
39. Jyotish NK, Singh LK, Kumar C (2023) Reliability assessment of safety-critical systems of nuclear power plant using ordinary differential equations and reachability graph. *Nucl Eng Des* 412:112469

Publisher's Note Springer Nature remains neutral with regard to jurisdictional claims in published maps and institutional affiliations.

Springer Nature or its licensor (e.g. a society or other partner) holds exclusive rights to this article under a publishing agreement with the author(s) or other rightsholder(s); author self-archiving of the accepted manuscript version of this article is solely governed by the terms of such publishing agreement and applicable law.